Correlation between the microstructure of mortar and replicated masonry walls

Additional Graduation Work
CIE 5050-09

Juan Felipe Garzón A
(4553004)

November 2017

Contents

List of Tables

List of Figures

1

Introduction

The Groningen gas field is located in the north of The Netherlands, being the largest in Europe and the tenth in the world. For several decades gas has been extracted from this area, nevertheless in the last years it has caused human-induced earthquakes which are believed to affect the existing structures in the region.

Nowadays, several research project are being done on the structural behavior of the masonry walls subjected to dynamic loads, although, another important aspect is to assess in an efficient way whether or not the existing masonry walls are susceptible to the seismic forces. In order to do it, a semi-destructive test based on microscopical technique is proposed. This methodology has been used in concrete structures for several years to evaluate the properties of the material and it has given reliable results showing that it is worth to do a feasibility study of the technique on the masonry walls

1.1. Objective

Due to need for finding a reliable semi destructive test to assess the exiting masonry structures in the region of Groningen, the aim of the project is to do a feasibility study on the relation between the microstructure of the mortar and the mechanical properties of replicated mason/ry walls and see if this technique can be applied to the existing structures on future researches.

1.2. Project plan

The project was divided into two parts. The first part involved the testing of ten replicated masonry walls which was done by the structural mechanics section. The walls were subjected to a four point bending test and the mechanical properties obtained were the flexural stress and the modulus of elasticity.

The second part was to obtain the composition of the microstructure of the mortar. For this, the used of polished and thin sections were considered, however, after one trial polish section was done it was noted that due to the high porosity of the cement paste and the size of the aggregates, the microstructure of the mortar could not be seen properly and the image analysis software was not going to work on it, therefore the thin sections were chosen as the best alternative for the research.

During the planning, the idea of comparing the microstructure of the bricks and the brick-mortar interface with the mechanical properties was considered, although, at the end the scope of the project didn't include these phases for the following reasons. In masonry walls the bricks are the strongest elements, which means that the global strength of the walls doesn't depend on them. As it can be seen in figure 2.1., in the flexural test the fracture develops in the mortar or the brick-mortar interface. Only in some cases, the bricks in the

top line fail due to the stress propagation of the wall

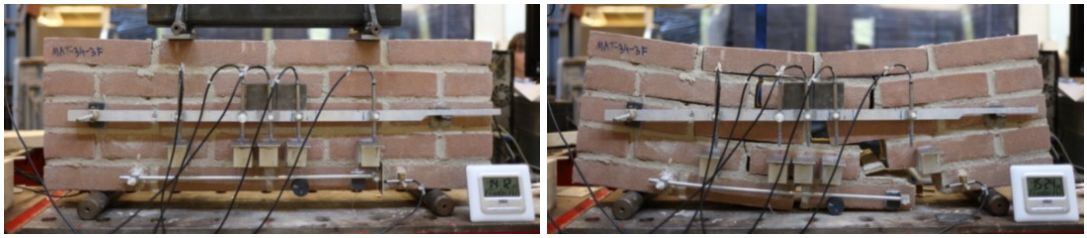

(a) (b)

Figure 1.1: (a) Assemblage masonry wall 3F (b) Failure masonry wall 3F.

The brick-mortar bond cannot be used for the correlation with the mechanical properties for several reasons. First, most of the factors mentioned by Groot [3] that affect the strength were not taking into account or controlled during the experimental phase (See section 2.1). Furthermore, in some of the samples there was a separation of the bricks and the mortar during the drilling phase, which can be seen in figure 1.2. The epoxy layer between the phases will affect the quantification of the voids in the mortar so the area cannot be taken into account. Also, the bonding pores were not consider as a representative variable since the number of specimens analyzed was limited.

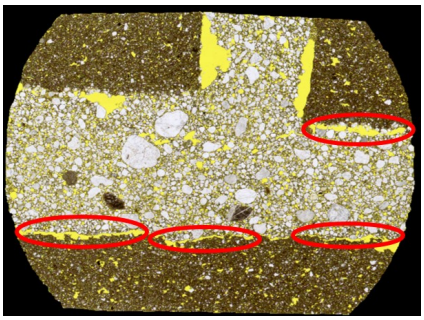

Figure 1.2: Affected interphase brick-mortar due to sample preparation

Finally the project plan is as follows:

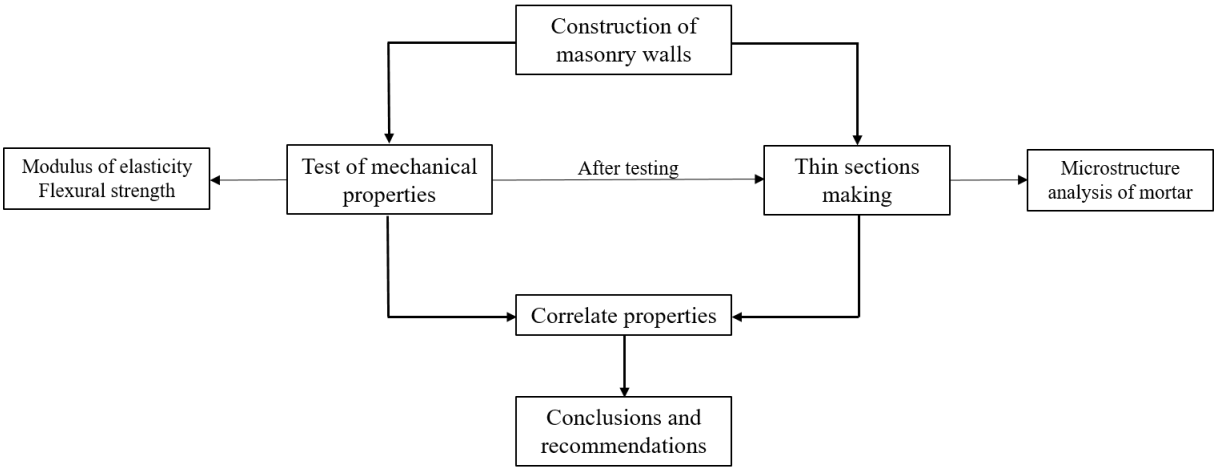

Figure 1.3: Project plan outline

2

Literature Survey

2.1. Masonry walls

Masonry is a construction material in which individual components such as clay or calcium silicate bricks are bind together with a lime or cement based mortar. The most common application is for the construction of walls for low rise buildings. It can be used as the structural system of a structure or also as protection or subdivision for a given space [4]. Similarly to concrete, masonry walls have a good compression strength but their tensile strength is low. For situations in which tensile forces are applied such as lateral forces [4] or soil settlements, the material will probably crack. This phenomenon happens in the masonry structures of Groningen that are subjected to the dynamic lateral forces.

The mortar content in masonry walls is around 7%. Nevertheless, its contribution to the strength of the element can be much higher than that [4]. The strength of the mortar can be affected by the loss of water after its placement, since the brick's porosity or humidity can increase or decrease the content [2]. In terms of the brick-mortar bond, a more porous brick will allow for a better mechanical bond between the components, but it can absorb more water from it increasing the amount of voids [1] affecting the bond quality. It can be seen that the properties of the mortar and the brick can affect in different ways the strength of the bond between them and of the wall itself. Table 2.1 summarizes the stablished the factors that can influence the brick-mortar bond strength[3].

			Properties influencing bong											
			Water flow	Water retention	Shrinkage	Bleeding	Volume changes on hydration	Degree of hydration	Porosity	Density of hydration products	Mechanical interlock-streucture	Chemical bond	Workability
Composition parameter	**Mortar**	Sand											
		Cement											
		Lime											
		Sand/cement ratio											
		Water/cement ratio											
		Water content											
		Air content											
		Additives											
	Brick	Porosity											
		Humdity											
		Chemical reactivity											
		Roughness of surface											
		Macro structure: Holes/form											

Table 2.1: Parameters that influence the brick-mortar bond in masonry walls

2.2. Mechanical properties and microstructure

In concrete, it is observed that the mix proportion is related to the fresh, hardened and durability properties of the material. The content of cement paste, capillary pores, coarse aggregate or fine aggregate can be correlated with properties such as the consistency, compression strength, tensile strength, modulus of elasticity and chloride or carbon penetration[6].

In the same way, the mortar parameters shown in table 2.1 affect its mechanical properties. The aggregates content, cement paste and voids of the mortar can be determine and it should give an indication of the properties of the mortar, and of the masonry walls.

3

Experimental program

The experimental program was divided into 4 stages, core drilling, sample preparation for the thin sections, image analysis and data analysis.

3.1. Core drilling

As mentioned earlier, the structural mechanics section is conducting their own study on masonry, therefore it was useful to use their walls for this research since the mechanical properties they obtained could be used for the correlation with the microstructure of the mortar. It is worth mentioning that the type of bricks, the mix design of the mortar and the construction of the walls was carried out by them.

The same mortar was used for all the masonry walls, it had a ready mix design in bags of 25 kg. Its components are shown in table 3.1. The amount of water of the mix was 3.7 liters per bag of mortar. The brick were clay bricks Euroa VB WF produced by Wienerberger.

Material	Quantity (kg)
Cement CEM1 42.5Rt	73.88
Water	182.24
Limestone filler	49.25
Hydrated lime CL80S1	110.82
Sand (0.00-1.20 mm)	775.76
Sand (1.20-3.55 mm)	221.64
Air entrained aditive	0.06
Water/Binder	0.78

Table 3.1: Mortar Mix Design for 1 m³

Once the specimens were tested, two or more cores were extracted from them. The location for the drilling was chosen randomly to avoid sampling bias, although, it was kept in mind that the spots had to be away from the affected parts of the walls, such as the failure cracks.

The extraction process was done without the use of water since this approach has proven to give good results in terms of the preservation of the sample, for instance it reduces the possibility of the splitting between the bricks and the mortar, although, during the process this happened with some samples.

3.2. Sample preparation

3.2.1. Primary epoxy impregnation

The cores were fully impregnated with a low viscosity epoxy to preserve the integrity of the samples and its microstructure during the process of mechanical sawing. Regarding masonry, the impregnation guarantees that there won't be any further splitting between the bricks and the mortar during the sample preparation.

The epoxy used was prepared using 3 different components, the low viscosity epoxy, a fluorescent epodye and the hardener. The use of fluorescent epodye has two functions, first its yellow color helps for the segmentation of the voids from the solid parts of the specimens. Also, it is essential for the UV light analysis of the sections, although, this tool was not used in the research, the technic can be apply for the prepared samples on future researches. The epodye has a mix proportion of 1 % w/w. Once both components are fully mixed, the new compound is mix with the hardener with a ratio of 1:3, so for 100 gr of epoxy, 30 gr of hardener will be used.

For the impregnation process, the samples were tightly packed in plastic bags with a tube attached which allowed the epoxy to get into them. Then, the samples were place in a vacuum impregnating chamber for 20 minutes. In the first 10 minutes the samples were subjected only to vacuum and in the remaining time (still under vacuum), they were impregnated guaranteeing that all the air voids were gone and that the epoxy got deep enough into the sample for a good confinement. Since the hardening of the epoxy is an exothermic reaction, after the impregnation the samples were submerged in cold water to control the increase of the temperature until the hardened was completed. Once the epoxy had fully hardened, the drilled cores were cut into slices of approximately 20 mm and then they were cut once again to fit the dimensions of the reference glass available, 30×45 mm. Figure 3.1 illustrates the primary epoxy impregnation procedure.

(a) (b) (c)

Figure 3.1: (a) Example of masonry core. (b) Masonry core after primary impregnation. (c) Slices masonry core.

3.2.2. Thin sections

Thin sections are defined as a 30 µm thickness samples since this value allows the properties of the material to be seen under the optical microscope and with the use of the Michel-Levy interference chart the desire features can be identify properly. Nevertheless, a thickness of 50-60 µm was chosen for the project since it provided a better contrast making it easier for the identification of the microstructure of the mortar. A detailed protocol for preparation of thin section has been written by Jakobsen [5]. A similar protocol was followed in achieving the thin sections. A total of 39 thin sections were analyzed, in general 3 samples per wall.

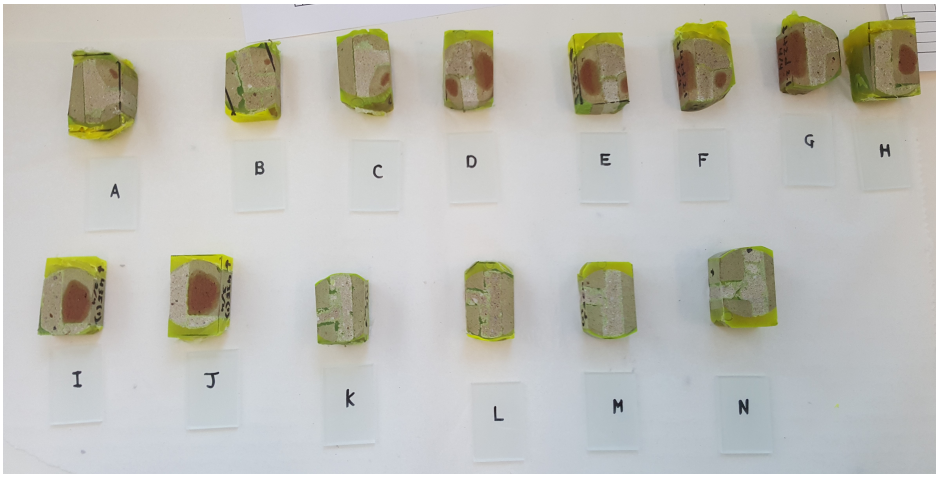

Figure 3.2: Masonry slices with dimensions 30 x 45 mm

The thin section making was divided into 2 parts and it was done using an automated machine. In the first part, the samples were glued to the reference glass using a part epoxy glue (plastic padding). Once the glue hardened, the reference glass was placed in the vacuum holder of the machine and the specimens were cut using a diamond blade to a thickness of 10.5 mm. After the cutting, the surface of the samples was not properly flat, therefore, it was grind it until a flat surface was achieved, which was done using a set of three diamond rollers, from coarse to fine. For a concrete sample, the grinding can take place right away after the cutting without any problems, nevertheless, if the masonry specimens were grind in the same way, due to their high porosity the material would have come off and the samples would have been damaged, for that reason their surfaces were first impregnated using the same procedure as in 3.2.1, guaranteeing that the epoxy protected and maintained the microstructure during the grinding process.

When the surface of the samples were flat, another impregnation was done with the purpose of having the epoxy into the microstructure for the recognition of voids and cracks (if present) during the analysis of the specimens. Since the epoxy would also cover the entire surface of the sample, the surface had to be grinded again with the finest roller to remove this layer. A full removal of the epoxy was guaranteed if the thickness of the sample was the same as the one before the impregnation.

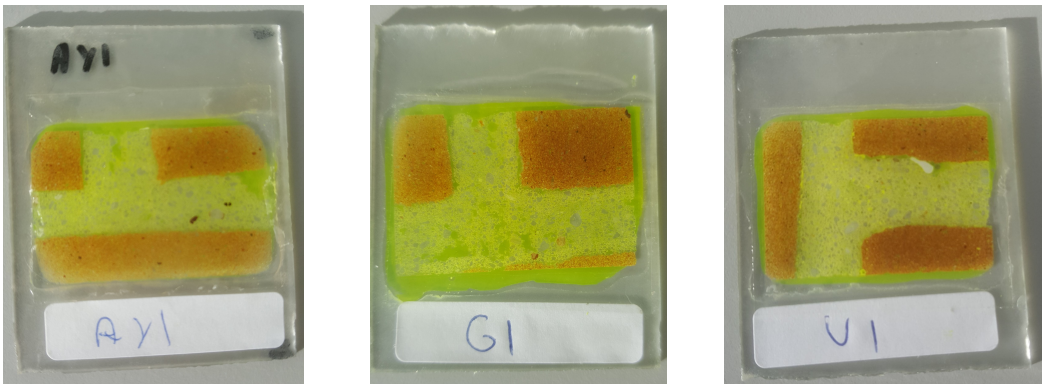

(a) (b) (c)

Figure 3.3: Examples of the final thin section

For the second part, a working glass with dimensions of 6.5×5.5×0.2 mm was glued to the im-

pregnated flat surface using UV-hardening glue. During this step, the glue had to be evenly distributed on the sample's surface since any irregularity would affect the final result. After the glue had hardened, the specimens were in between the reference glass and the working glass. The working glass was placed in the vacuum holder and the samples were cut with the diamond disc to a thickness of 0.5-0.7 mm. Since the surface would have been uneven as before, the procedure in step 1 was repeated to flatten it.

The grinding process was done until the thickness of the samples was around 50-60 µm. To ensure that the samples were good, their thickness was measured in different zones and by scanning them it was checked if the different phases could be identified by the image analysis software. After the checks, using the UV-hardening glue, a cover class was glued to the surface of the sample to protect it from abrasion and environmental effects such as carbonation. Examples of the final thin sections are shown in figure 3.3.

3.3. Image analysis

The images were scan using an Epson V800 photo scanner with an image resolution of 3200 dpi ($8\,\mu m/pixel$). The work was carried out using a JAVA based open source image analysis software called ImageJ (Fiji). The image analysis process was divided into 4 steps.

3.3.1. Primary segmentation

Before the segmentation, the images were scaled using the resolution from the scanner. Later, using red color, RGB value (255, 0, 0), the mortar parts were segmented from the thin sections as it is shown in figure 3.4. The criteria for choosing the color was completely arbitrary, the only parameter was that it should be completely different from the colors in the mortar to avoid any troubles with the identification of the phases.

The interface brick-mortar was also colored since the study of its properties were not included in the scope of the project. This zone was defined as the area in which the mortar was not homogeneous, for instance in figure 3.5 there are big voids present due to the separation of the bricks and the mortar in the drilling phase.

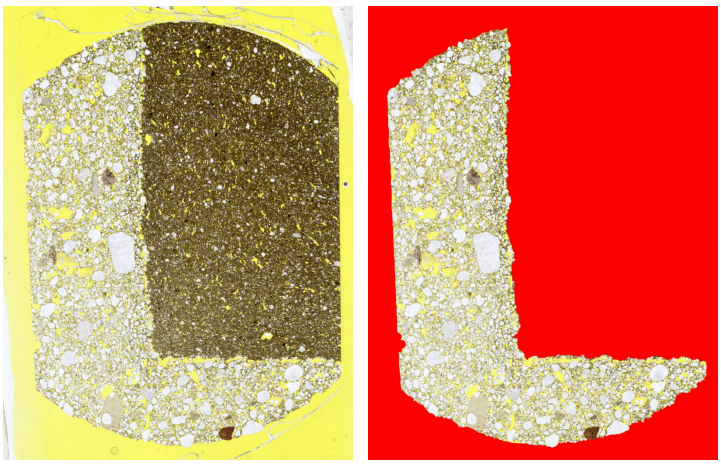

(a) (b)

Figure 3.4: (a) Original thin section. (b) Segmented mortat phase.

3.3.2. Image Classifier

For the segmentation of the images, a plugin based on machine learning from Image J called Weka was used. The general idea is that a classifier was trained and then it was used to segment the images.

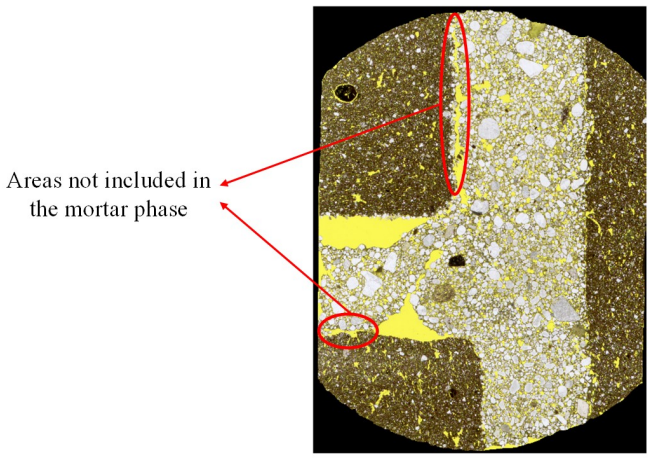

Figure 3.5: Affected interface brick-mortar

The software offers several training features, after trying the most relevant ones, it was decided that the Gaussian blur gave the more reliable results with a low computational time. Before starting the training, the categories in which the user desires to segment the images had to be created. To segment the mortar 4 categories were create, Voids, Aggregates, Paste and Red, the first three represent the phases of the material and the latter the empty parts of the picture.
To segment the images, the user had to classify manually some pixels into the established categories. With the input data, the classifier learned about the pixels classification and used the training feature to predict the category of the non-classify pixels and segment the entire picture. As a rule of thumb, the more manually classified pixels the better the segmentation, nevertheless this procedure would have been very time consuming, instead, it was wise to classify a few pixels and let the software classify the image. Probably, the first results was not going to be very accurate, but then the software allowed the user to know which pixels were more difficult to classify, so he could focus on those and get a good classifier and segmentation in less time.

3.3.3. Image Segmentation

For the image segmentation, a couple of steps were done in advance. Since some of the samples had different thickness due to the sample preparation, this had a direct impact on the tone of its color. As shown in figure 3.6, a thicker section had darker colors and a better contrast while the thinner ones had clear colors and a low contrast. This doesn't mean that the samples were not useful but that more hours had to be invested since several classifiers were need it due to the differences of pixel values in the images. In order to use less classifiers, after the primary segmentation was done, the contrast of the images was improved using the function *Enhnace constrat* with the *equalize histogram* option check. The software stretched the histograms, making them more similar between each other. See figures 3.7 (a) and (b). A few images were still too different to use the same classifiers, so different ones were used for some particular cases.

The aggregate phase had two issues for the segmentation procedure, in contrast with the white/clear gray color of the majority of the particles, some had a brownish tone and/or had inside voids or dark color traces. The latter problem was solved after the segmentation was done so it will be explain in detail in the following paragraphs.

For the first problem, the classifier understood that the brownish pixels correspond to the paste phase, therefore it would assume that those dark aggregates would be also paste. One can tell the classifier that the brown aggregates were indeed aggregates, but then it would confused the pixel values of the aggregates and the paste. An easier solution was to manually

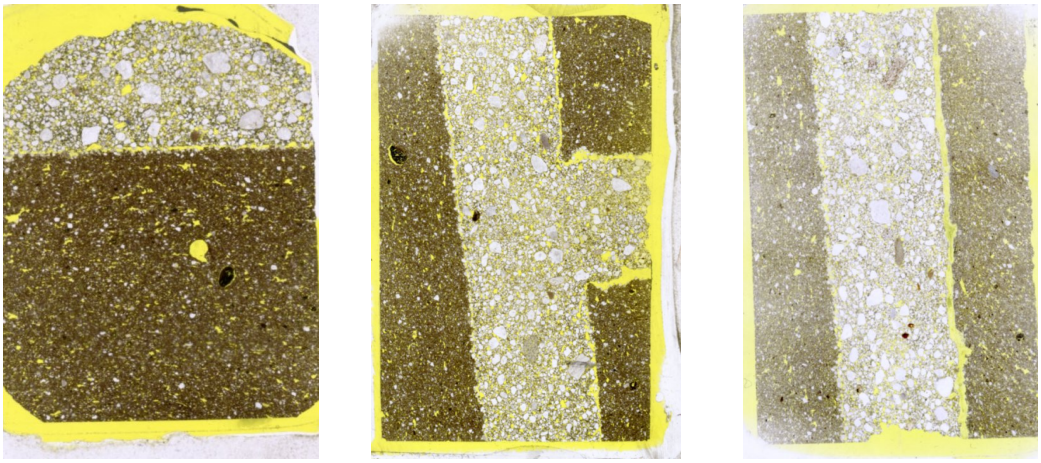

(a) (b) (c)

Figure 3.6: From left to right, the thickness of the thin sections decreases, affecting the constrast of the images.

color the aggregates with the same pixel values of the rest of the particles, by doing this, also the second problem was partially solved, although that one was fully solved at a later stage. It's important to say that since the brown aggregates vary in size, some of the small particles might not have been colored because the user would have missed them, nevertheless the impact of it on the final results can be neglected. Figures 3.7 (b) and (c) show the difference after the aggregates have been colored.

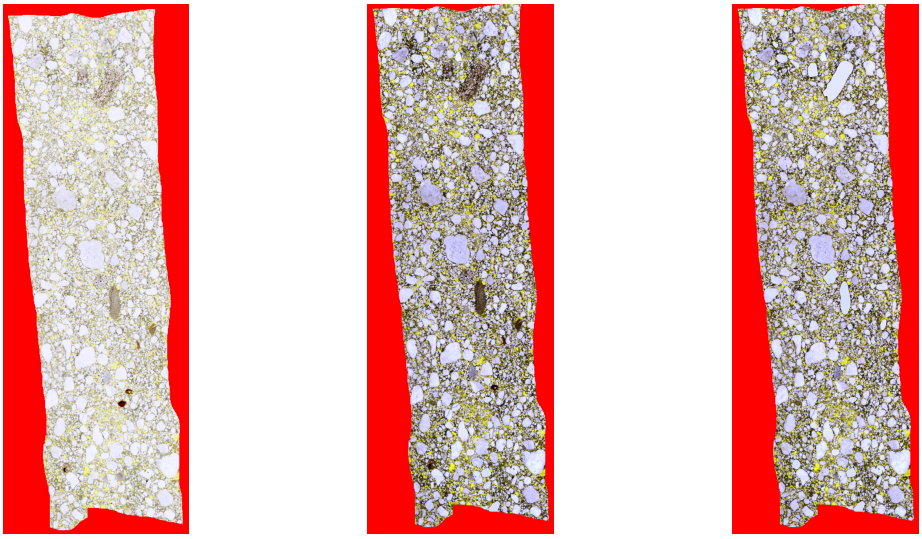

(a) (b) (c)

Figure 3.7: (a) Original mortar. (b) Mortar after applying the function *Enhnace contrast*. (c) Mortar after coloring the brownish aggregates.

Once the contrast of the images was adjusted and the aggregates were colored, the classifier was applied and the images were segmented. The software turned the images into a N color images, being N the number of categories defined. The mortar image would have 4 different colors. At this stage, the histogram of the images changed to a 4 bars, so the percentages of every phase could be obtained immediately. Nevertheless, if that was done at this point, the porosity and the dark traces of some aggregates would have been included in the porosity and the paste of the mortar respectively. To solve the problem, the image was turned into an 8 byte, then using the threshold tool of the software the aggregates were selected, turning the image into binary. With the binary function *fill holes*, the aggregates were filled

solving the void and dark traces problem. Using the menu of *Image calculator*, function *MIN*, from the segmented image and the binary aggregates a new image that distinguish accurately all the phases of the mortars was obtained. The final result of the segmentation is shown in figure 3.8

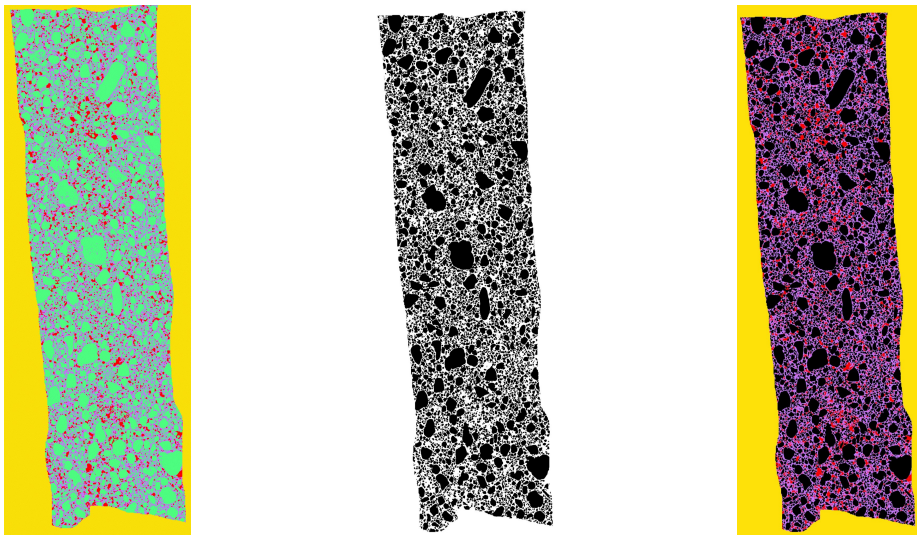

(a) (b) (c)

Figure 3.8: (a) Original segmeneted Weka image. (b) Binary image of aggregates after using the function *fill holes*). (c) Final image for the mortar composition

3.4. Data analysis

As mention earlier, during the sample preparation the masonry could get damaged because of the sawing and grinding process. The damages were reflected as large voids either in the mortar-brick interface or within the mortar. Since those voids were not present at the moment of the test of the walls, they couldn't be taken into account for the quantification of the voids of the mortar. The threshold used to define the large voids was 1 mm of Feret diameter, only the voids below this value were taken into account. Finally, using this threshold, the mortar composition, aggregates, cement paste and voids, was obtained from the final images in 3.3.3. To compute the mortar composition of each wall, a weighted average of the images was done. Other examples of segmented images are shown in figure 3.9.

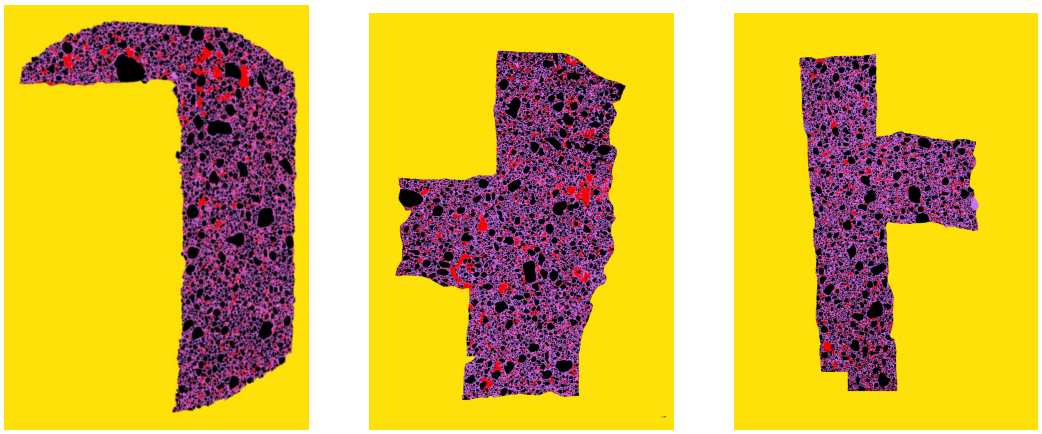

(a) (b) (c)

Figure 3.9: Examples of segmented images

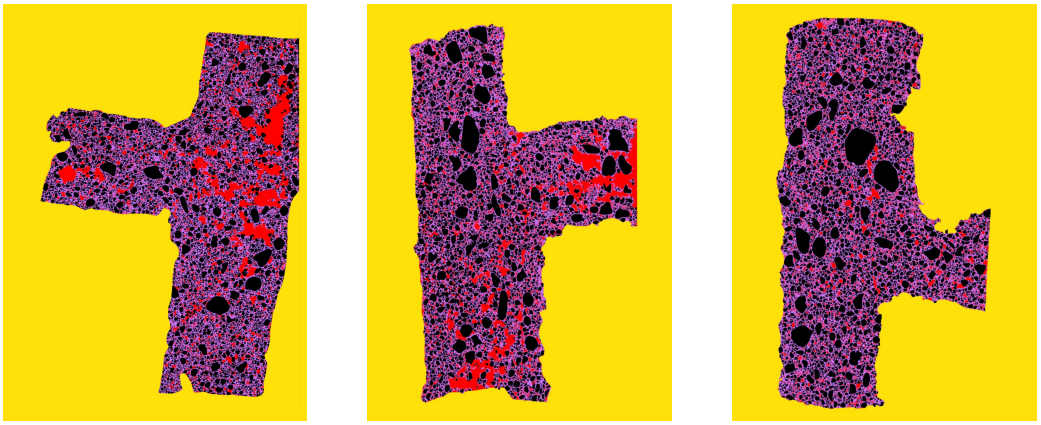

(d) (e) (f)

Figure 3.9: Examples of segmented images

4

Results

4.1. Mechanical properties

The results are divided into two parts, the properties of the bricks and mortar used separately, and two batches of walls, the first with three walls and the second with seven walls. The first batch of walls had double line of brick for its thickness and only the flexural strength was measured. In the second batch, the walls had a single line of bricks and the flexural strength and the modulus of elasticity were measured.

Table 4.1 and 4.2 show the mechanical properties of the bricks and mortar individually and of the masonry walls respectively.

Material	Compressive stength	Flexural strength
Clay Brick	28.31	2.74
Mortar	3.82	1.40

Table 4.1: Mechanical properties bricks and mortar

	42A	42D	42E	3A	3B	3C	3D	3E	3F	3G
Modulus of elasticity (N/mm²)	-	-	-	1977	3125	1962	1344	2404	1665	2087
Flexural strength (N/mm²)	0.18	0.17	0.09	0.27	0.55	0.31	0.23	0.28	0.24	0.60

Table 4.2: Mechanical properties masonry walls

4.2. Mortar composition

After the segmentation of the images, the composition of the single mortar mix design was obtained:

	42A	42D	42E	3A	3B	3C	3D	3E	3F	3G
Voids (%)	11	15	15	10	11	9	9	10	11	9
Aggregates (%)	52	51	53	51	51	51	52	54	53	54
Paste (%)	37	34	32	39	37	40	39	36	36	37

Table 4.3: Mortar composition

4.3. Correlation

Since the mortar composition within the different walls didn't have the same values, one can said that the mechanical properties of those areas are locally different. Nevertheless, the flexural strength and the modulus of elasticity were measured for the entire wall assuming that the elements were homogeneous. Therefore, the same assumption was done for the mortar microstructure, it remained constant for each wall. Finally, the correlation with the mechanical properties was done with the mean values of the mortar composition.

As it can be seen in the columns of the left in graphs 4.1 and 4.2, on a first approach the correlation was done using all the data available from the mechanical properties and the mortar microstructure. For the flexural stress, in graphs (k) and (g) the value of R^2 was 0.0037 and 0.32 respectively. On a similar trend, for the E modulus, in graphs (c) and (i) the value of R^2 was 0.00 and 0.27 respectively.

Assuming that a good correlation has an R^2 value of at least 0.60, the correlations obtained were quite low, therefore, it was decided to remove arbitrary some walls from the graph in order to get the best possible correlation. In the case of the flexural strength it was decided to remove maximum 4 walls while in the modulus of elasticity maximum 2 since in the first one there was more data available. Table 4.4 shows the walls that were remove for each case. In particular, walls 3B and 3G were excluded since their mechanical properties were considerably high in compare of the rest of the elements. The analysis of the results is explained in the following sections.

	Flexural strength	Modulus of elasticity
Voids	3B, 3G	3B, 3D
Aggregates	3A, 3B, 3C, 3G	3A, 3B
Paste	3B, 3C, 3G	3B, 3F
Voids/Aggregates	3B, 3C, 3G	3C, 3F
Voids/Paste	42a, 3B, 3C, 3G	3C, 3F
Aggregates/Paste	42e, 3B, 3E, 3G	3A, 3B

Table 4.4: Walls remove to improve the correlation

4.3.1. Flexural stress

Table 4.5 shows the increment of the R^2 coefficient after the removal of the data from table 4.4. Regardless of the differences between the increments of the R^2 , in both scenarios the Voids and Voids/Aggregates ratio had the higher R^2 while Paste and Aggregates/Paste ratio the lowest, showing that independently of the R^2 value, some of the mortars phases correlate better than the others with the flexural strength.

	Initial R^2	Improved R^2	Ratio
Voids	0.29	0.65	2.24
Aggregates	0.15	0.55	3.67
Paste	0.079	0.37	4.68
Voids/Aggregates	0.32	0.71	2.21
Voids/Paste	0.20	0.63	3.15
Aggregates/Paste	0.003	0.40	108.11

Table 4.5: Initial R^2 and Improved R^2 for the flexural strength.

Since the parameters related to the voids content had an R^2 higher than 0.60, they are considered to have a good correlation with the flexural strength. As shown in graphs 4.1 (a), (b), (g), (h), (i) and (j), there is an inverse relation between the void content and the flexural strength of the walls while in graph 4.1 (e) and (f) there is a direct relation between the cement

paste and the flexural strength.

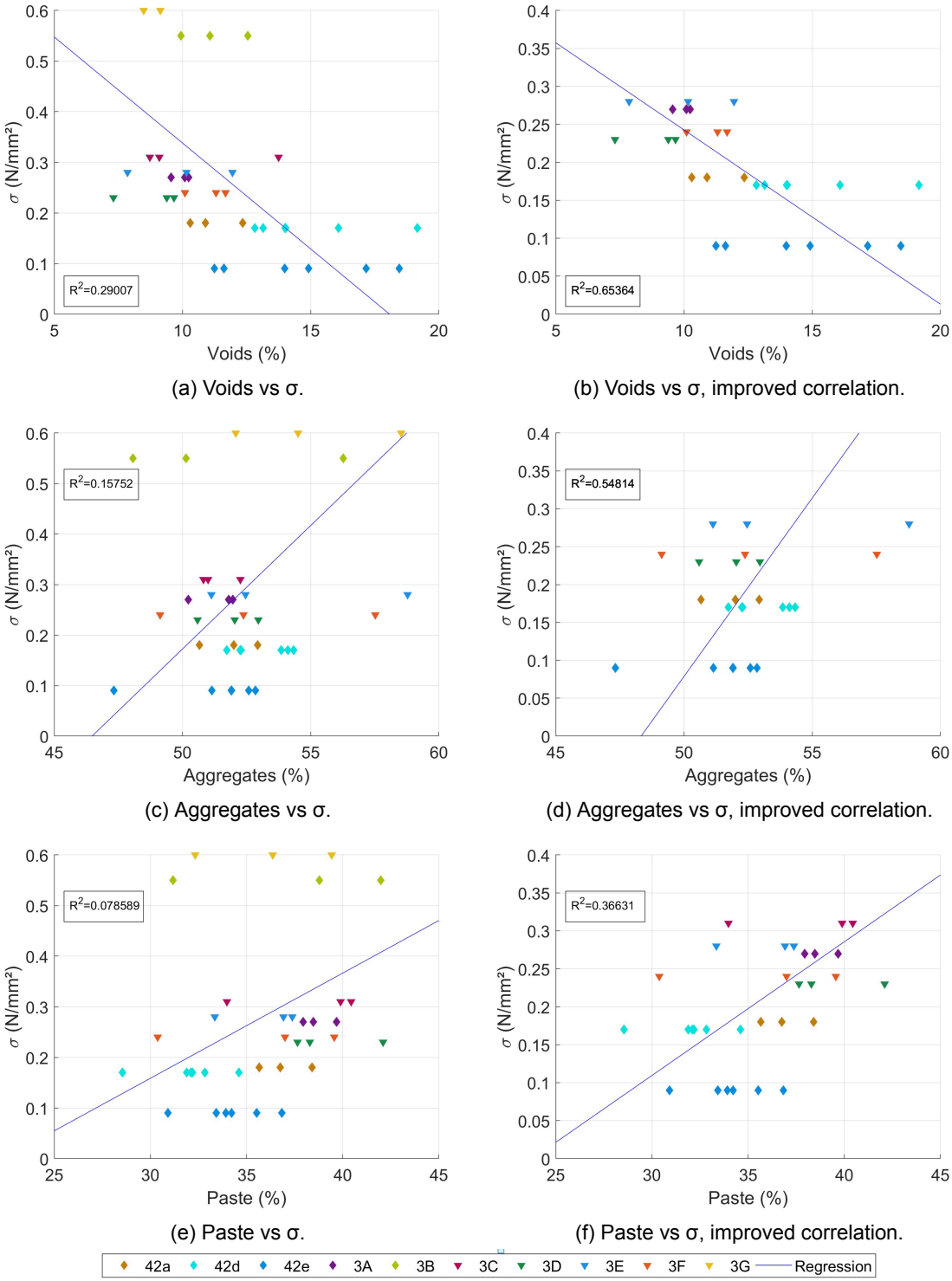

(a) Voids vs σ.

(b) Voids vs σ, improved correlation.

(c) Aggregates vs σ.

(d) Aggregates vs σ, improved correlation.

(e) Paste vs σ.

(f) Paste vs σ, improved correlation.

Figure 4.1: Correlation between the microstructure parameters and maximum flexural stress, σ.

Assuming a constant amount of water in the mix design, an increment in the cement paste is due to a higher content of unhydrated cement in the original mix design which means a lower W/C for the global design. A mix designs with low W/C will have less voids and a higher strength, therefore it can be seen that the behavior between graphs 4.1 (a), (b), (e), (f), (i) and (j) is logical.

In compare with graphs 4.1 (e) and (f), in graphs (c) and (d) it can be said that an increment in the aggregates content has a higher influence in the flexural strength than an increment in the cement paste, probably because of the fact that the high porosity of the cement paste makes it weaker in compare of the aggregates, so the latter has a larger contribution in the mortar strength and the masonry walls themselves.

Assuming a constant content of aggregates, in graphs 4.1 (g) and (h), a lower amount of voids implies a higher content of cement paste meaning that the flexural strength should be higher as the correlation obtained shows. Since the aggregates contribute more to the strength of the mortar, for a constant content of voids, if the aggregate content reduces, it will mean that the cement paste will increase, and since the latter is weaker, the flexural strength of the walls will decrease. Nevertheless, when it is compared with the voids, it is clear that an increment of the cement paste will increase the strength of the mortar as mention earlier. Graph 4.1 (l) shows a different relation as described before, for a constant

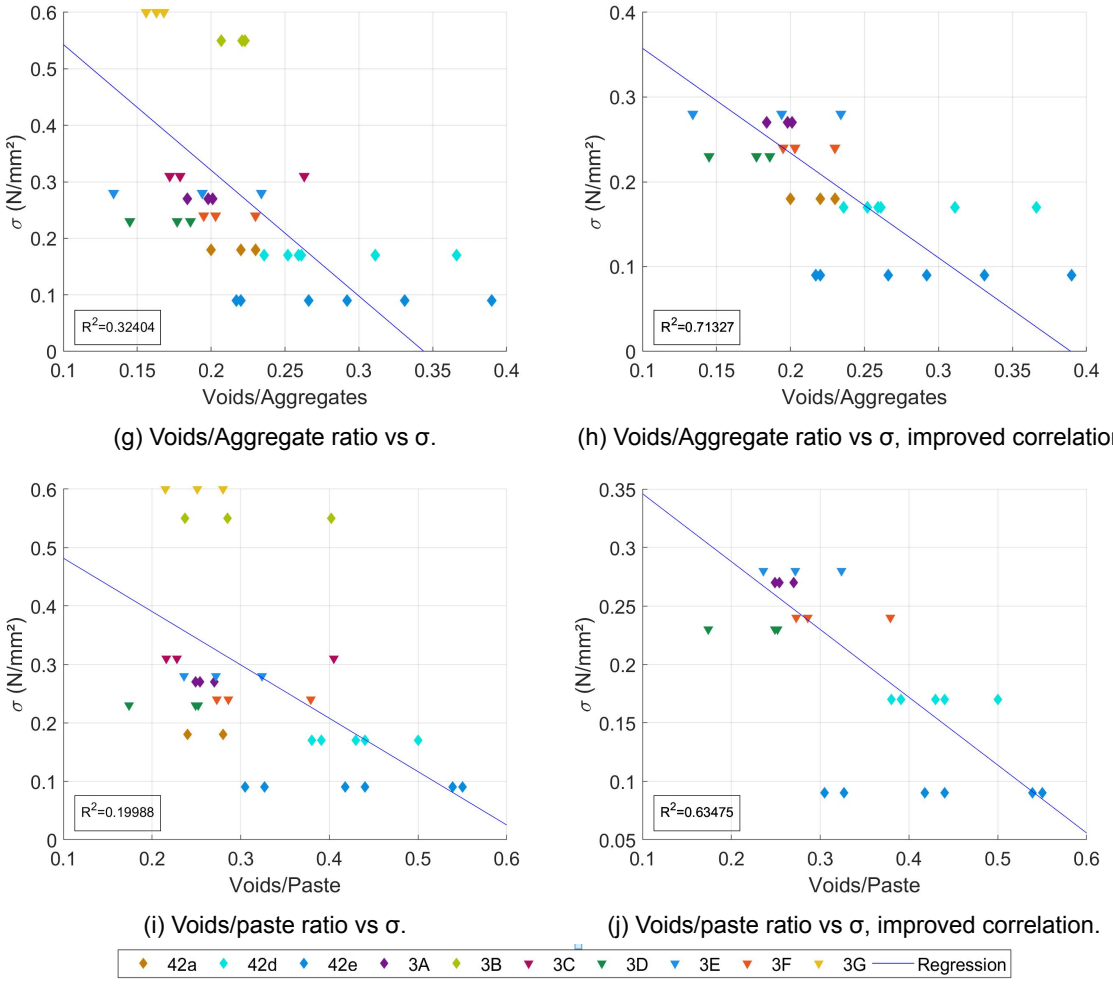

(g) Voids/Aggregate ratio vs σ.

(h) Voids/Aggregate ratio vs σ, improved correlation.

(i) Voids/paste ratio vs σ.

(j) Voids/paste ratio vs σ, improved correlation.

Figure 4.1: Correlation between the microstructure parameters and maximum flexural stress, σ.

amount of paste, a reduction of the aggregates will implied an increment of the voids which reduces the flexural strength, nevertheless the graph shows the opposite behavior. On the other hand, for a constant amount of aggregates an increment in the paste will increase the strength, which is logical since the amount of voids will reduce. Although, it is important to remember that at the beginning graph 4.1 (k) didn't have a correlation and after removing walls 42e, 3B, 3E, 3G, there was a trend in graph 4.1 (l), but still in compare with the others

parameters, this one has one of the lowest R^2.

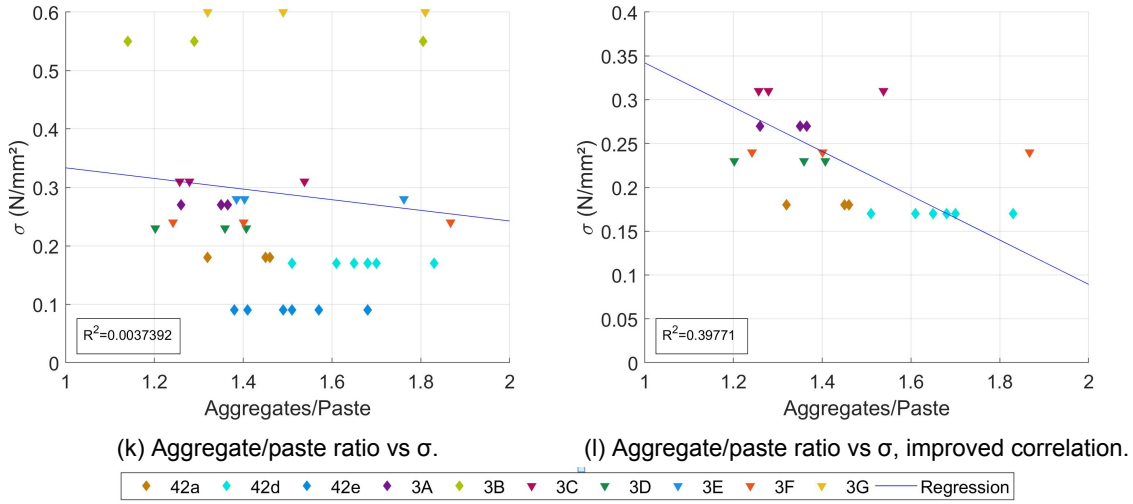

(k) Aggregate/paste ratio vs σ.

(l) Aggregate/paste ratio vs σ, improved correlation.

Figure 4.1: Correlation between the microstructure parameters and maximum flexural stress, σ.

4.3.2. Modulus of elasticity

Table 4.5 shows the increment of the R^2 coefficient after the removal of the data from table 4.4.

	Initial R^2	Improved R^2	Ratio
Voids	0.25	0.31	1.24
Aggregates	0.0001	0.35	3500
Paste	0.089	0.69	7.75
Voids/Aggregates	0.21	0.30	1.42
Voids/Paste	0.27	0.28	1.02
Aggregates/Paste	0.04	0.35	8.75

Table 4.6: Initial R^2 and Improved R^2 for the modulus of elasticity

In compare with the with the flexural strength, the correlation with the modulus of elastic and the microstructure of the mortar was lower, one of the reason can be that there was less data or that the mortar properties just correlate better with the flexural strength, to clarify this, more data is required.

For the improved correlation, it can be said that the voids, aggregates and paste parameters on their own have the higher correlation with the modulus of elasticity, although only the latter has an R^2 higher than 0.60, therefore only the paste content correlates good enough with the modulus of elasticity.

As it can be seen in graphs 4.2 (a) to (d) and (g) to (j), the relation between the variables changed after the removal of the data, for instance, in graph 4.2 (a) there is contradictory behavior between the voids and the modulus of elasticity, since a higher content of voids implies less amount of material reducing the E modulus. On a first approach, some variables where remove and an R^2 of 0.79 was obtained, although it had the same trend as graph (a). Since this was wrong, another data was selected and the correlation obtained had an R^2 of 0.31 as shown in graph 4.2 (b). The same thing happened with the other graphs, therefore, one must be careful at the moment of removing the desire data since it can completely change the trend between the parameters even if it improves the R^2 value.
For the aggregates and paste content, graphs 4.2 (c), (d), (e) and (f) show a logical relation.

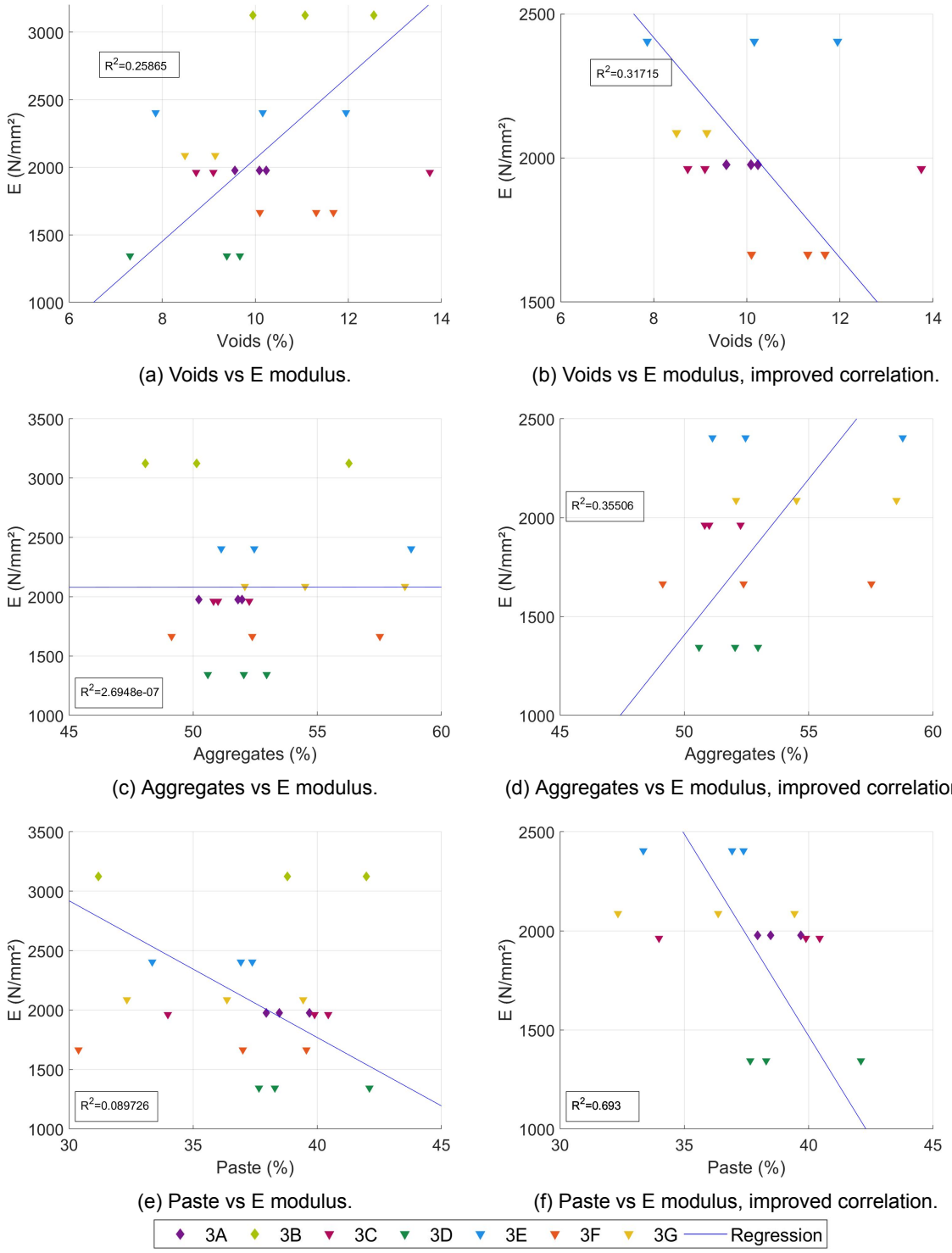

(a) Voids vs E modulus.

(b) Voids vs E modulus, improved correlation.

(c) Aggregates vs E modulus.

(d) Aggregates vs E modulus, improved correlation.

(e) Paste vs E modulus.

(f) Paste vs E modulus, improved correlation.

Figure 4.2: Correlation between the microstructure parameters and modulus of elasticity, E

Since aggregates have a higher modulus of elasticity than mortar, an increase on it will increase the stiffness of the composite material, while the cement paste has a lower modulus of elasticity so the effect will be the opposite, an increment of it will reduce the stiffness of the mortar. For the aggregate content, there a similar case as for graphs 4.2 (a) and (b), by removing the right data from graph 4.2 (c) there was an important improvement between the correlation of the aggregates and the E modulus as it is shown in graph 4.2 (d).

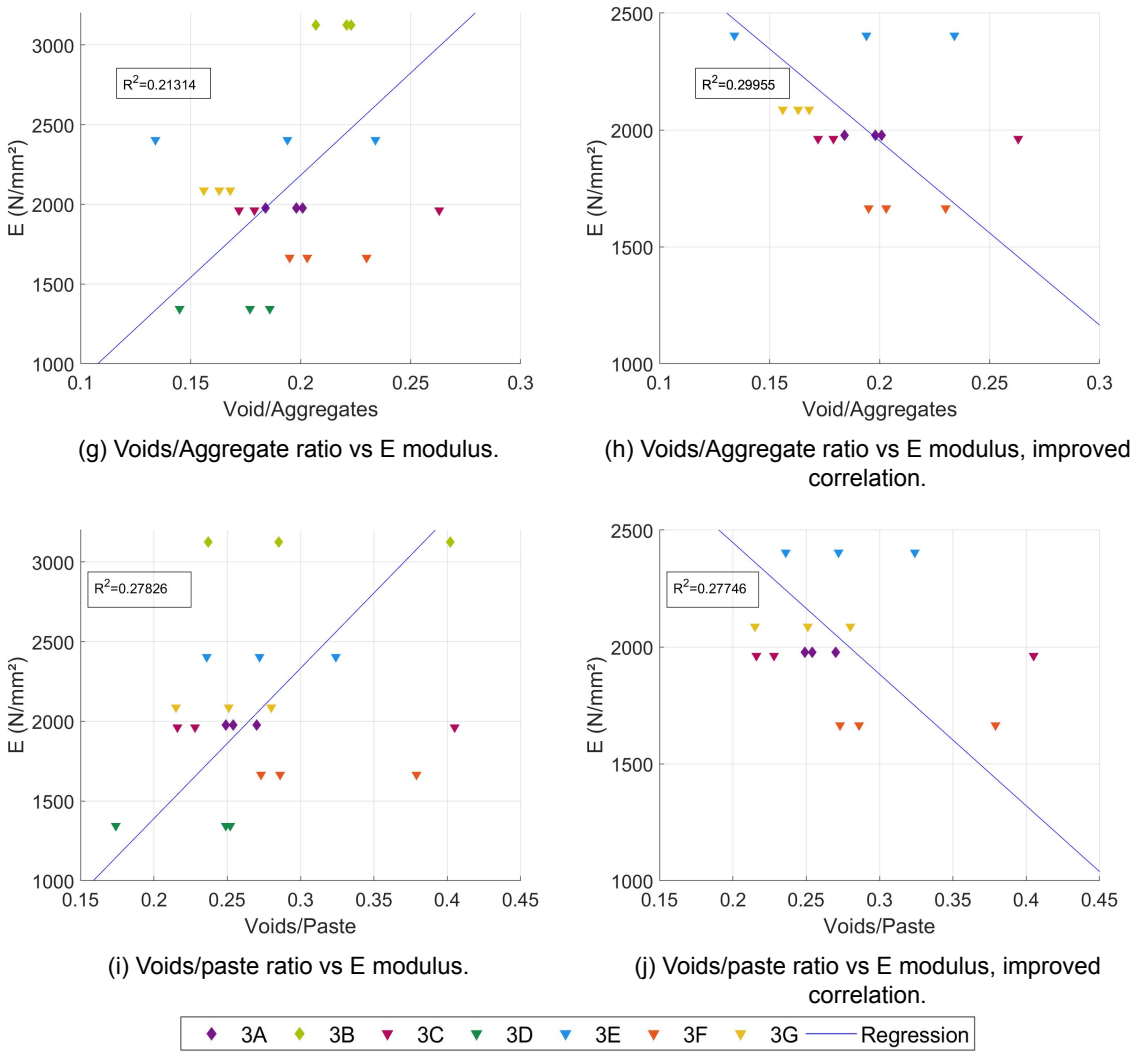

(g) Voids/Aggregate ratio vs E modulus.

(h) Voids/Aggregate ratio vs E modulus, improved correlation.

(i) Voids/paste ratio vs E modulus.

(j) Voids/paste ratio vs E modulus, improved correlation.

Figure 4.2: Correlation between the microstructure parameters and modulus of elasticity, E

For a constant amount of aggregates and paste, graphs 4.2 (h) and (j) respectively show the same behavior as graph 4.2 (b) for the void content, an increment in the voids content will decrease the Modulus of elasticity since less material will be available. On the other hand, assuming a constant amount of voids, an increment of the aggregates content in graph 4.2 (h) will increase the Modulus elasticity as it was seen in graph 4.2 (d). On the contrary, in graph 4.2 (j), for a constant amout of voids an increment in the paste implies a reduction of the aggregate content meaning that the E modulus should reduce, nevertheless it increases showing a behavior different from graph different (f).

Finally, graphs 4.2 (k) and (l) show that for a constant amount of paste, an increment in the aggregates content increases the modulus of elasticity as in graph 4.2 (d), and on the other case, for a constant content of aggregates and increment in the cement paste should increase the modulus of elasticity since the amount of voids are reducing, although this is not shown in the graph.

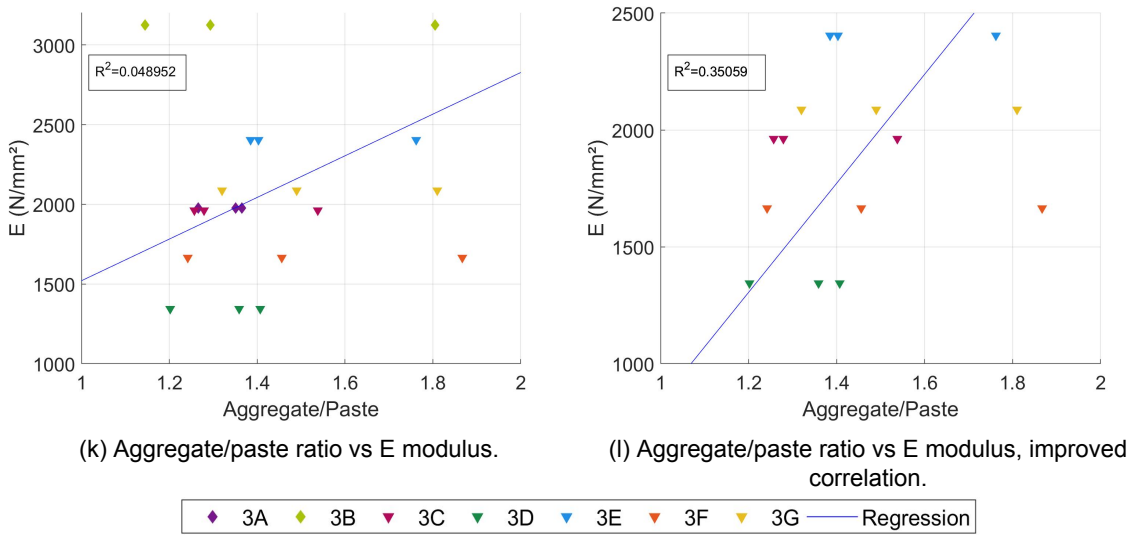

(k) Aggregate/paste ratio vs E modulus.

(l) Aggregate/paste ratio vs E modulus, improved correlation.

Figure 4.2: Correlation between the microstructure parameters and modulus of elasticity, E.

5

Conclusions and Recomendations

5.1. Conclusions

The feasibility study shows that even using one single mortar mix design, its microstructure can be correlated with the flexural strength and modulus of elasticity of the replicated masonry walls. It is possible to think that with further research a semi destructive test to estimate the mechanical properties of the existing walls based on this technique can be implemented. This could predict not only the strength of the walls against the different loads, but also the strains it can resist before it cracks which can be useful in case of settlements.

Since the scope of the project included only one type of mortar, it could be said that it was expect that its microstructure was in general similar along the masonry walls. Nevertheless, the results showed a variability in the properties of the mortar probably due to the skills of the workers or the properties of the bricks which are intrinsic aspects in the construction method of the elements.

Furthermore, at first it can be seen that the flexural strength correlates better than the modulus of elasticity with the microstructure of the mortar, nevertheless, it is important to keep in mind that for the first there was more data available, therefore more data is required to established if this is true or not.

The Voids, Voids/Aggregates and Voids/Paste have a good a correlation (R^2 higher than 0.60) with the flexural strength, so one can said that by controlling or measuring the amount of voids in the mortar the flexural strength of the masonry walls could be estimated. On the other hand, the amount of paste is the only parameter that correlates good with the modulus of elasticity.

5.2. Recomendations

Since the research was done with only one mortar mix design, the use of different mix designs that provide low and high strengths is of interest. If there is more data available, it will give a better correlation for all the variables and it could be possible to established the influence of the mortar phases in the mechanical properties of the walls. For instance, it can be expected that a high strength mortar will have a low content of voids and a high cement paste content making the walls stronger and stiffer.

On the other hand, the structural mechanics department has performed two types of non-destructive test for the bricks and mortar of the masonry walls, the ultrasonic test and the Hammer Schmidt test, therefore it is worth to analyze if the results from the mortar can be correlated with the ones present in this document.

The scope of the project was limited to replicate masonry walls built in the lab, therefore

it will be of interest to include samples from the existing masonry walls in Groningen and compare those results with the ones obtained under lab conditions.

6

Acknowledgements

First of all, I would like to thank the *Nederlandse Aardolie Maatschappij* (NAM) for sponsoring this research, I hope the results presented in this document will be useful for you. I also want to thank my supervisors Dr. Oguzhan Copuroglu and Dr. Henk Jonkers for their help and guidance along this process, it allowed me to improve not only the final version of this document but also my personal knowledge and skills.
Furthermore I want to thank the Structural Mechanics department for providing me the results from their mechanical test, I also hope that these work can be useful for their current and future researches. Finally I want to thank Ameya Kamat for his help and hard work during the sample preparation stage which allowed us to make 39 thin sections.

Bibliography

[1] N Beningfield, N Winter, and S Farrell. An interim investigation into pore formation in masonry mortar and the use of microscopy to investigate the probable initial air content. *Masonry International*, 25(1):9, 2012.

[2] Caspar Johannes Wilhelmus Petrus Groot. Effects of water on mortar-brick bond. *HERON, 40 (1, 1995*, 1995.

[3] CJWP Groot. Aspects of mortar-brick bond. *Brick and Block Masonry(8 th IBMAC) London, Elsevier Applied Science,*, 1:175–181, 1988.

[4] Emeritus AW Hendry. Masonry walls: materials and construction. *Construction and Building materials*, 15(8):323–330, 2001.

[5] UH Jakobsen, P Laugesen, and N Thaulow. Determination of water-cement ratio in hardened concrete by optical fluorescence microscopy. *Special Publication*, 191:27–42, 1999.

[6] Povindar Kumar Mehta. Concrete. structure, properties and materials. 1986.